Enhanced deep ultraviolet emission from Si-doped $Al_xGa_{1-x}N$/AlN MQWs

2010 Chinese Phys. B 19 127801

(http://iopscience.iop.org/1674-1056/19/12/127801)

Enhanced deep ultraviolet emission from Si-doped $Al_xGa_{1-x}N$/AlN MQWs*

Li Da-Bing(黎大兵)[a)b)†], Hu Wei-Guo(胡卫国)[b)], Miyake Hideto(三宅秀人)[b)], Hiramatsu Kazumasa(平松和政)[b)], and Song Hang(宋 航)[a)]

[a)] *Key Laboratory of Excited State Processes, Changchun Institute of Optics, Fine Mechanics and Physics, Chinese Academy of Sciences, Changchun* 130033, *China*

[b)] *Department of Electrical and Electronic Engineering, Mie University, Tsu* 514-8507, *Japan*

(Received 27 January 2010; revised manuscript received 19 February 2010)

Undoped and Si-doped AlGaN/AlN multiple quantum wells (MQWs) were grown on AlN/Sapphire templates by metalorganic phase vapor epitaxy. High-resolution x-ray diffraction measurements showed the high interface quality of the MQWs little affected by Si-doping. Room-temperature (RT) cathodoluminescence measurements demonstrated a significant enhancement of the RT deep ultraviolet emission at about 240 nm from the AlGaN/AlN MQWs by Si doping. The mechanism of the improved emission efficiency was that the Si-doping partially screens the internal electric field and thus leads to the increase of the overlap between electron and hole wavefunctions. Further theoretical simulation also supports the above results.

Keywords: nitride, quantum wells, optical properties, luminescence

PACC: 7800, 7865, 8100, 8115H

1. Introduction

Deep ultraviolet (DUV) optoelectronic devices based on III-nitrides with emission wavelength below 340 nm have attracted much attention because of their many promising potential applications in environmental, biological and information fields, such as air–water purification, biosensors and non-line-of-sight communication, high density storage, and so on.[1] However, at present, the efficiency of DUV devices, especially DUV light emitting diodes (LED), is much lower than that of blue devices.[2] Several methods have been reported to improve the efficiency of the DUV devices by different researchers.[3−5] Khan's group has developed a migration enhanced epitaxy metal organic vapor phase epitaxy (MOVPE) technique and strain manage engineering to reduce the defect formation and thus to obtain quite high-quality MQWs with high Al-content, which results in an enhancement of DUV emission.[3] Growth of AlGaN/AlN MQWs on AlN bulk substrate by conventional MOVPE has also obtained high emission intensity at 260 nm.[4] Also it has been reported a significant increase of the 280-nm DUV cathodoluminescence (CL) emission from the AlGaN MQWs due to the formation of AlGaN quantum dots in the well region.[5] Taking the advantage of high quality Al-rich MQWs, it is essential to obtain highly efficient DUV emission by decreasing the effect of internal polarization field. Recently, it has been reported that strong emission intensity can be realized by optimizing the well width of Al-rich MQWs to weaken the internal polarization field effect.[6] However, the most attractive method is the fabrication of the nitride-based DUV devices on non-polar or semi-polar homo-substrates.[7,8] At present, there are some technical obstacles on growing high-quality and large-area non-polar or semi-polar homo-substrates and thus there is a long way to go on fabricating devices on non- or semi-polar bulk substrates. In this study, we proposed another approach, i.e. doping engineering, mainly Si-doping, to control the internal polarization electric field in the MQW active

*Project supported by the National Natural Science Foundation of China (Grant No. 60976011), the Knowledge Innovation Program of CIOMP (Grant No. 08CY32M080), the Akasaki Research Center at Nagoya University, Japan, the Grants-in-Aid for Scientific Research of the Ministry of Education, Culture, Sports, Science and Technology of Japan (Grant Nos. 18360008 and 18560010), and the Scientific Research on Priority Areas of the Ministry of Education, Culture, Sports, Science and Technology of Japan (Grant No. 18069006).

†Corresponding author. E-mail: lidb@ciomp.ac.cn

region of the DUV-LEDs to enhance the DUV emission. This approach has been proved to be effective in case of InGaN/GaN MQWs and GaN/AlGaN.[9,10] Our CL measurements confirm a great improvement of the DUV emission at about 240 nm from the MQWs with Si-doping.

2. Experimental

Six periods AlGaN/AlN MQWs were grown by MOVPE on 1-μm thick AlN/Sapphire template. A set of Si-doped AlGaN/AlN MQWs with different dopant position was grown to investigate the influence of Si-doping on the structure and optical properties of AlGaN/AlN MQWs. The growth temperature and pressure for all samples were 1180 °C and 40 Torr (1 Torr=133 Pa), respectively. TMA, TMG, CH_3SiH_3 and ammonia (NH_3) were used as the source of Al, Ga, Si and N, respectively. High-resolution x-ray diffraction (XRD) and cathodoluminescence (CL) were employed to characterize the structure and optical properties of the MQWs.

3. Results and discussion

Figure 1 shows the reciprocal space maps of (10–15) reflections of the AlGaN/AlN MQWs without and with Si-doping in well layers. The inclined dashed line represents stress free reciprocal lattice points and the vertical dashed line stands for coherent reciprocal lattice points. According to Fig. 1, the coherence does not change with doping; moreover, besides the zero peak and ±1st satellite peak, a weak –2nd satellite peak is also observed for the MQWs with Si-doping in well layers. But for the MQWs without doping, besides the zero peak, only a weak –1st is observed. Thus, the Si-doping can improve the interface quality of the MQWs in certain degree. Furthermore, the well and barrier width are extracted to 6 nm and 7 nm and the Al-content is about 0.7 from the XRD measurements.

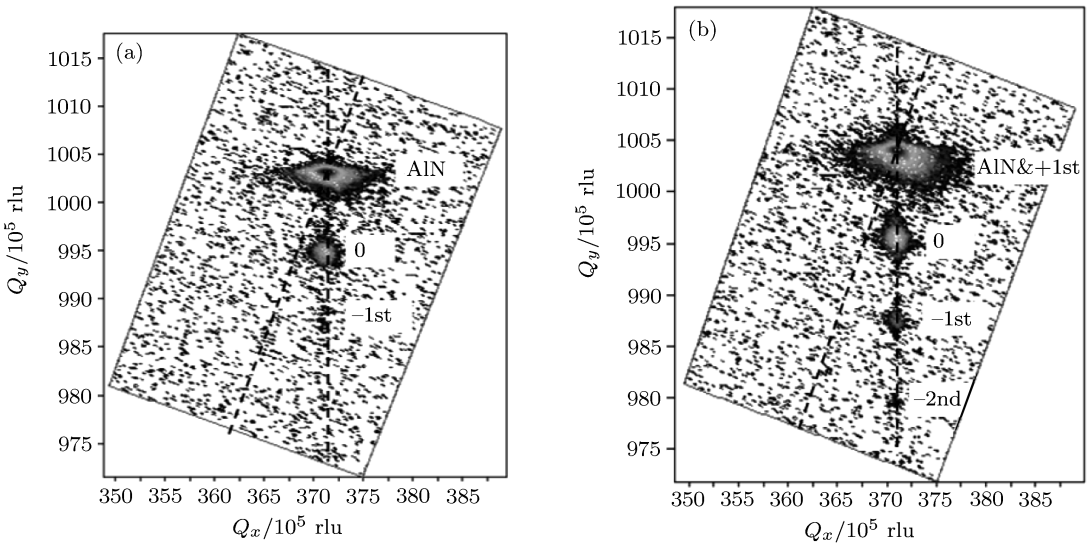

Fig. 1. Reciprocal space maps of (10–15) reflections of the AlGaN/AlN MQWs (a) without Si-doping and (b) with Si-doping in well layer.

Figure 2 depicts the room-temperature (RT) CL spectra of the AlGaN/AlN MQWs with different dopant positions. For comparison, the inset of Fig. 2 shows the CL spectra of undoped and well-doped AlGaN/AlN MQWs. The CL intensity is enhanced with Si-doping, especially for the dual-doped MQWs, for which the CL intensity is drastically improved. The enhancement of CL spectra with Si doping is attributed to the increasing overlap between the electron and hole wavefunctions since the internal polarization electric field has been screened by carriers originating from the Si doping. Further measurements under different E-beam current of CL have been carried out (Fig. 3). It can be seen that the emission peaks of

AlGaN/AlN MQWs shift to high energy side with increasing E-beam current. The quantity of shift is different for different dopant positions. With increasing the E-beam current, the shift is 30 meV for the well-doped MQWs, 21 meV for the barrier-doped MQWs and 12 meV for the dual-doped MQWs, which implies that the internal polarization electric field is different for different dopant positions, that in the dual-doped MQWs it is the smallest, and in the barrier-doped MQWs it is smaller than that in the well-doped MQWs.

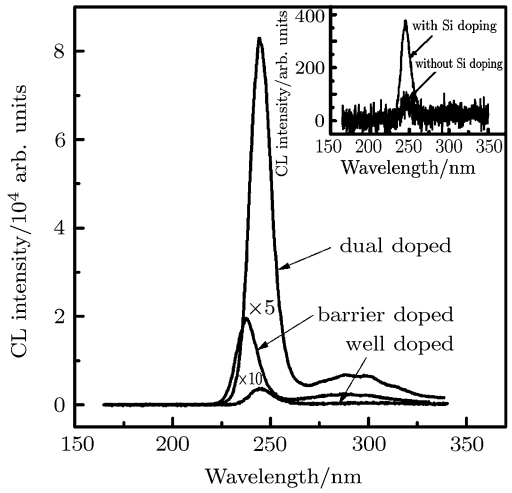

Fig. 2. CL spectra of the AlGaN/AlN MQWs with Si-doping in different positions. The inset shows the CL spectra of undoped and well-doped AlGaN/AlN MQWs.

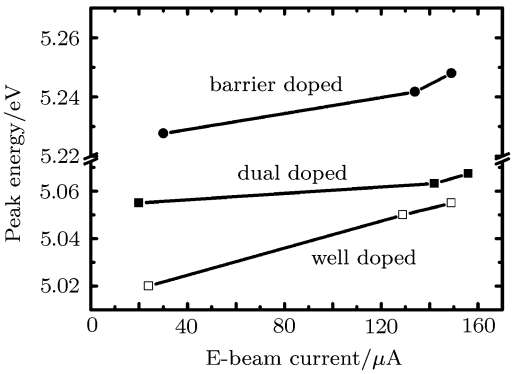

Fig. 3. Dependence of peak energy of the AlGaN/AlN MWQs on the E-beam current of CL.

To further explore the physical mechanism of the Si-doping effects on optical property of the AlGaN/AlN MQWs, the MQWs band diagram is calculated by solving the Poisson–Schrödinger system of equations self-consistently using the method of finite differences. The process is as follows: we simply consider a twofold degenerate valence band consisting of heavy and light holes of the same isotropic effective mass. The eigenenergies $E^i_{\rm c,v}$ and envelope $\psi^i_{\rm c,v}$ of the electron and hole subbands can be calculated from the one-dimensional (1D) effective-mass Schrödinger equation:

$$\left[-\frac{\hbar^2}{2}\frac{\rm d}{{\rm d}z}\frac{1}{m^*_{c,v}(z)}\frac{\rm d}{{\rm d}z}+V_{\rm c,v}(z)\right]\psi^i_{\rm c,v}(z)=E^i_{\rm c,v}\psi^i_{\rm c,v}(z),$$

where $m^*_{\rm c,v}$ are the electron and hole effective mass, respectively, and the conductor-band discontinuity $\Delta E_{\rm c}=(0.7)\Delta E_{\rm g}$.[11] The potential energy is given by

$$C_{\rm c,v}(z)=\Delta V_{\rm c,v}(z)+V_{\rm H}(z)+V_{\rm xc}(z),$$

where $V_{\rm c,v}(z)$ are the edges of conduction and valence bands in bulk host-materials, respectively; $V_{\rm H}(z)$ is the Hartree term of the potential energy due to non-uniform carriers distribution; $V_{\rm xc}(z)$ is the exchange–correlation potential. The exchange–correlation potential $V_{\rm xc}(z)$ can be calculated in the framework of the local density approximation (LDA) in the Kohn–Sham density functional theory (DFT).[12] To obtain the Hartree potential it is necessary to solve Poisson's equation:

$$\varepsilon_0\frac{\partial}{\partial z}\varepsilon(z)\frac{\partial}{\partial z}\phi(z)=-e_0(p(z)-n(z)+N^i_d(z)-N^i_a(z))+\sigma(z)\delta(z-z_i),$$

where $p(z)$, $n(z)$ are the hole and electron concentrations; $N^i_{\rm d}(z)$, $N^i_{\rm a}(z)$ are the ionized donor and acceptor dopant concentrations respectively.

The dependence of the ionized dopant concentration on the temperature can be found by the following formulae:

$$N^i_{\rm d}(z)=\frac{N_{\rm d}(z)}{1+2\cdot{\rm e}^{(F_{\rm c}+E_{\rm d})/k_{\rm B}T}},$$

$$N^i_{\rm a}(z)=\frac{N_{\rm a}(z)}{1+4\cdot{\rm e}^{(F_{\rm v}-E_{\rm a})/k_{\rm B}T}},$$

where $N_{\rm d}(z)$, $N_{\rm a}(z)$ are the donor and acceptor concentrations; $F_{\rm c}$, $F_{\rm v}$ are the Fermi quasi-levels for the electrons and holes; $E_{\rm d}$, $E_{\rm a}$ are the ionization energies of donors and acceptors respectively; T is the lattice temperature. To calculate the charge concentration, $p(z)$, $n(z)$, $N^i_{\rm d}(z)$, and $N^i_{\rm a}(z)$, the Fermi energy should be known. Some authors have suggested an imaginary Fermi energy. And we take the charge balance condition, suggested by B. Gogai to determine the Fermi energy,[13] which can describe our phenomena more accurately:

$$p(z)-n(z)+N^i_{\rm d}(z)-N^i_{\rm a}(z)=0.$$

Especially, it is worth while noting that $\sigma(z)$ is the sheet charge induced by the piezoelectric polarization $P_{\rm piezo}$ and spontaneous polarizations $P_{\rm spont}$ which is the intrinsic cause that separates hole and electron envelop to decrease the internal quantum efficiency,

$$\sigma(z) = P_{\rm piezo} + P_{\rm spont}.$$

The spontaneous polarization is determined by the material properties, and the XRD ω–2θ scan results are used to calculate the stress in the MQWs and then to deduce the piezoelectric polarization. The related parameters can be found in Refs. [14] and [15] and the results are exhibited in Fig. 4. The polarization charge induces high internal field as large as 2.25 MV/cm, which makes the energy band inclining. Under the effect of the field, the free charge (electron and hole) accumulates at the energy lowest-point and highest-point, respectively, which induces a static potential opposite to polarization field to bend energy structure and thus partially screens the polarization field. The degrees of bending and screening are determined by the accumulated charge density. Our simulations reveal that only when the charge density is larger than 1×10^{19} cm^{-3}, can the energy structure show distinct bending, which is similar to the simulation results of GaN/AlGaN.[15] Then, in undoped AlGaN/AlN MQWs, the energy band forms a typical triangle force structure and electron and hole wavefunctions are spatially separated, which greatly reduces the transition probability (Fig. 4). For 1×10^{20} cm^{-3} Si doping in well, the energy band in well is bent distinctly by the static potential which partly screens the polarization fields. At the same time, the energy-band still keeps quasi-linear in the barrier. However, with the same concentration of Si doped in the barrier, the energy structures in both the well and the barrier are bent greater and the screen effect of static charge is larger. Due to larger effective mass, the hole wavefunction localization by the polarization fields is very weak so that the wavefunction slightly moves towards the centre, which enhances the overlaps of electron and hole wavefunction. The Fiorentini results also prove that hole wavefunction is hard to be localized in AlGaN/GaN MQWs.[16] Dual-doping further screens the polarization field and the energy is close to the flat-band structure. The transition energy of the highest hole level and lowest electron level is shown in Fig. 5.

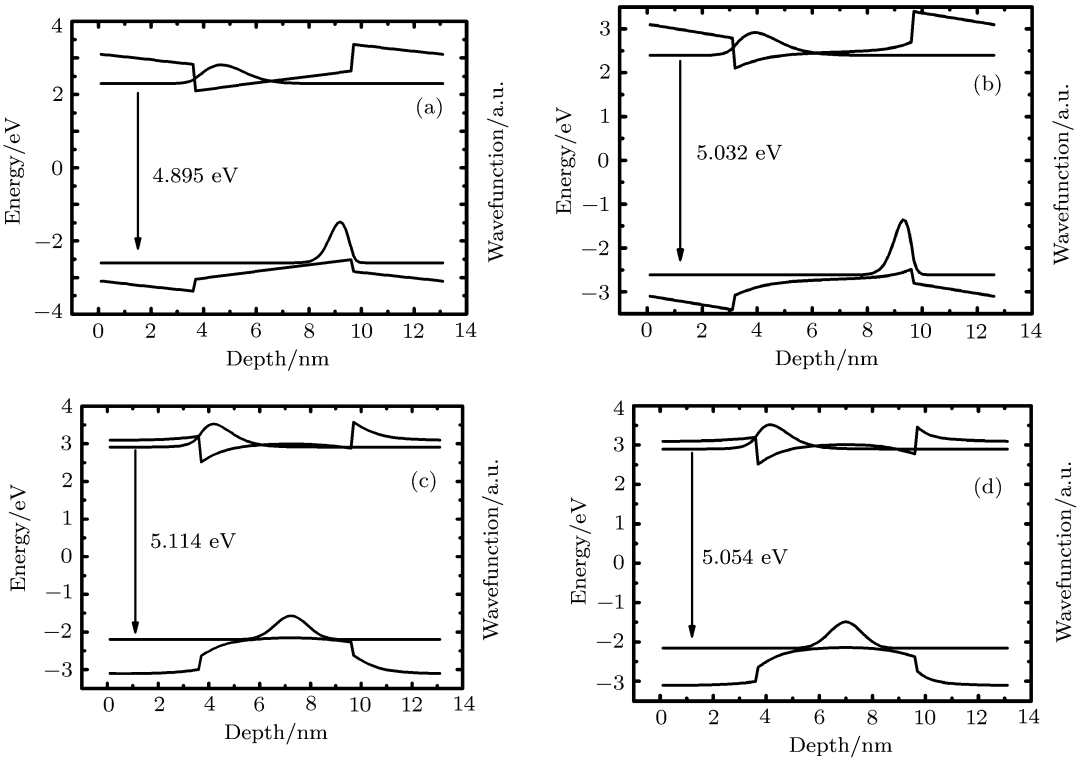

Fig. 4. Energy band structure and wavefunction of (a) undoped MQWs; and (b) well-doped MQWs; (c) barrier-doped MQWs; (d) dual-doped MQWs.

The simulations well fit with the CL measurement results: the well-doped sample has shift to high energy side and the dual-doped sample has larger shift, and the barrier-doped sample has the largest shift. This phenomenon is attributed to the screen effect of high concentration charges induced by doping. The slight difference in values mainly due to the calculation error and measurement errors. Additionally, the non-equilibrium carrier charges induced by the CL measurements are excluded in our simulations, which is another factor causing the difference between the simulations and CL measurements. The transition probability is the squared overlap of the electron and hole wavefunctions,[17,18] and then the product of highest hole level and lowest electron level wavefunctions is exhibited in Fig. 5.

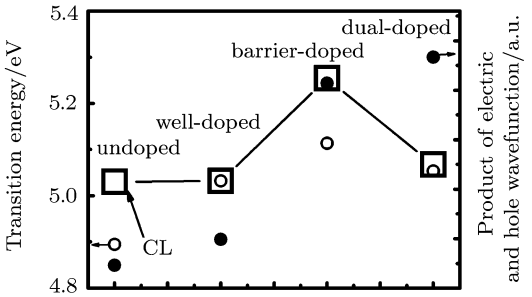

Fig. 5. The transition energy of the highest hole level and lowest electron level, the wavefunction product and the peak energy measured by CL.

The well doping increases the transition probability. And the barrier doping greatly increases the transition probability because the hole localization is weakened and the wavefunction moves towards the centre of MQWs. At last, the transition probability is further enhanced in dual-doped MQWs. This result is basically in agreement with the CL measurements.

4. Conclusion

Undoped and Si-doped AlGaN/AlN MQWs were grown by MOVPE. The effect of Si-doping in different positions of the MQWs was investigated by HRXRD and CL. The HRXRD results showed that the AlGaN/AlN MQWs have high interface quality and Si-doping has no obvious influence on the crystalline quality of the MQWs. RT–CL measurements demonstrated a significant enhancement of the RT deep UV emission at about 240 nm for the AlGaN/AlN MQWs with Si doping. The mechanism of the improvement of luminescence efficiency was interpreted by partial screening of the internal polarization electric field by the Si-doping and thus resulting in the increasing of the overlap between the electron and hole wavefunctions. Furthermore, the MQWs band diagram was calculated by solving the Poisson and Schrödinger equations; and the simulation showed that the energy band begins to bend at a doping concentration of 1×10^{19} cm^{-3}, which further evidenced the reliability of ours.

References

[1] Khan M A 2006 *Phys. Stat. Sol.* A **203** 1764

[2] Nakamura S and Fasol G 1997 *The Blue Laser Diodes* (New York: Springer)

[3] Zhang J P, Khan M Asif, Sun W H, Wang H M, Chen C Q, Fareed Q, Kuokstis E and Yang J W 2002 *Appl. Phys. Lett.* **81** 4392

[4] Gaska R, Chen C, Yang J, Kuokstis E, Khan A, Tamulaitis G, Yilmaz I, Shur M S, Rojo J C and Schowalter L J 2002 *Appl. Phys. Lett.* **81** 4658

[5] Borisov B, NiKishin S, Kuryatkov V and Temkin H 2005 *Appl. Phys. Lett.* **87** 191902

[6] Tahtamouni T M Al, Nepal N, Lin J Y, Jiang H X and Chow W W 2006 *Appl. Phys. Lett.* **89** 131922

[7] Tahtamouni T M Al, Sedhain A, Lin J Y and Jiang H X 2007 *Appl. Phys. Lett.* **90** 221105

[8] Sun W H, Yang J W, Chen C Q, Zhang J P, Gaevski M E, Kuokstis E, Adivarahan V, Wang H M, Gong Z, Su M and Khan M Asif 2003 *Appl. Phys. Lett.* **83** 2599

[9] Ryu M Y, Yu J, Shin E J, Yu P W, Lee J I, Yu S K, Oh E S, Nam O H, Sone C S, Park Y J and Kim T I 2000 *Solid Sate Commun.* **116** 675

[10] Hirayama H and Aoyagi Y 1999 *MRS Internet J. Nitride Semicond. Res.* **4S1** G3.74

[11] Martin G, Botchkarev A, Rockett A and Morkoç H 1996 *Appl. Phys. Lett.* **68** 2541

[12] Städele M, Majewski J A, Vogl P and Görling A 1997 *Phys. Rev. Lett.* **79** 2089

[13] Jogai B 2002 *J. Appl. Phys.* **91** 3721

[14] Lee K S, Yoon D H, Bae S B, Park M R and Kim G H 2002 *ETRI Journal* **24** 270

[15] Vurgaftman I and Meyer J R 2003 *J. Appl. Phys.* **94** 3675

[16] Fiorentini V, Bernardini F, Sala F D, Carlo A I and Lugli P 1999 *Phys. Rev.* B **60** 8849

[17] Carlo A D, Pescetelli S, Paciotti M, Lugli P and Graf M 1996 *Solid State Commun.* **98** 803

[18] Carlo A Di 1998 in *Tightbinding Approach to Conputational Materials Science* ed. Turchi P E A, Gonis A and Colombo L 1998 *MRS Symposium Proceedings* **491** 389